JACC: BASIC TO TRANSLATIONAL SCIENCE VOL. 5, NO. 1, 2020

PRECLINICAL RESEARCH

Stabilizing Peri-Stent Restenosis Using a Novel Therapeutic Carrier

Patrick H. Kee, MD, PhD,[a] Melanie R. Moody, BSc,[a] Shao-Ling Huang, PhD,[a] Hyunggun Kim, PhD,[a,f] Xing Yin, MD, PhD,[a] Tao Peng, MD,[a] Susan T. Laing, MD,[a] Melvin E. Klegerman, PhD,[a] Mohammad H. Rahbar, PhD,[a,b] Deborah Vela, MD,[e] Curtis Genstler, MD, PhD,[d] Kevin J. Haworth, PhD,[c] Christy K. Holland, PhD,[c] David D. McPherson, MD[a]

VISUAL ABSTRACT

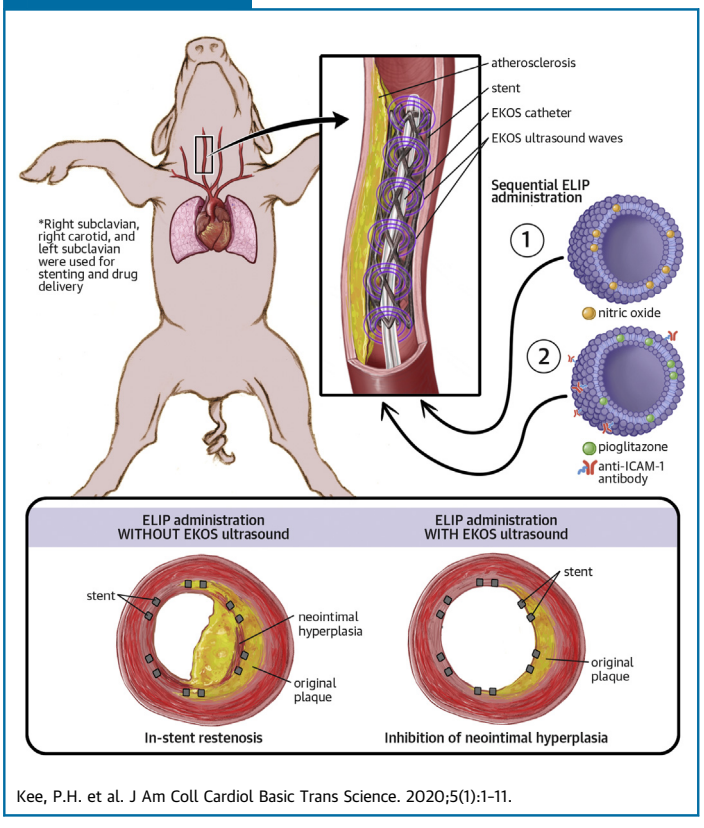

Kee, P.H. et al. J Am Coll Cardiol Basic Trans Science. 2020;5(1):1–11.

HIGHLIGHTS

- **Late in-stent restenosis is a significant problem in the management of atherosclerotic arterial disease that has not been completely ameliorated by the use of drug-eluting stents.**
- **ELIPs have been developed by our laboratory for specific ligand targeting, payload encapsulation, and ultrasound-activated payload release.**
- **An EndoSonic endovascular catheter with an ultrasonic core approved by the U.S. Food and Drug Administration for ultrasound-assisted, catheter-directed thrombolysis was harnessed to deliver and activate our ELIP preparations for targeted drug delivery in the peri-stent atheroma.**
- **Two ELIP preparations, nitric oxide–containing ELIPs and anti–intercellular adhesion molecule-1 antibody–conjugated, pioglitazone-loaded ELIPs, were sequentially delivered and ultrasonically activated by an EKOS catheter in stented arteries in an atherosclerotic miniature swine model.**

ISSN 2452-302X https://doi.org/10.1016/j.jacbts.2019.09.005

ABBREVIATIONS AND ACRONYMS

ELIP = echogenic liposome

ICAM = intercellular adhesion molecule

IVUS = intravascular ultrasound

NO = nitric oxide

PGN = pioglitazone

SPDP = 3-(2-pyridyldithio propionic acid)-*N*-hydroxysuccinimide ester

- **This study presents in vivo evidence of ELIP targeting to inflamed arterial wall by anti-intercellular adhesion molecule-1 antibody and ultrasound-driven pioglitazone delivery into deeper layers of the arterial wall. The result is a marked decrease in atheroma formation in the peri-stent region in arteries where the ultrasound-activated therapeutic was administered.**

SUMMARY

Late in-stent restenosis remains a significant problem. Bare-metal stents were implanted into peripheral arteries in miniature swine, followed by direct intra-arterial infusion of nitric oxide–loaded echogenic liposomes (ELIPs) and anti-intercellular adhesion molecule-1 conjugated ELIPs loaded with pioglitazone exposed to an endovascular catheter with an ultrasonic core. Ultrasound-facilitated delivery of ELIP formulations into stented peripheral arteries attenuated neointimal growth. Local atheroma-targeted, ultrasound-triggered delivery of nitric oxide and pioglitazone, an anti-inflammatory peroxisome proliferator–activated receptor-γ agonist, into stented arteries has the potential to stabilize stent-induced neointimal growth and obviate the need for long-term antiplatelet therapy. (J Am Coll Cardiol Basic Trans Science 2020;5:1–11) © 2020 The Authors. Published by Elsevier on behalf of the American College of Cardiology Foundation. This is an open access article under the CC BY-NC-ND license (http://creativecommons.org/licenses/by-nc-nd/4.0/).

In the management of atherosclerotic lesions, stent implantation is effective against acute luminal loss, but the potential for late luminal loss due to in-stent restenosis remains an important clinical challenge (1). Neointimal growth and in-stent restenosis are the results of acute arterial injury by angioplasty, platelet and leukocyte activation due to stent component exposure, and smooth muscle cell proliferation (2,3). Stents delivering antiproliferative agents such as sirolimus and paclitaxel are effective against neointimal proliferation, but the unpredictable risk of very late stent thrombosis due to impaired re-endothelialization and delayed vascular healing remains a significant problem (4,5). Despite the success of drug-eluting stents in reducing in-stent restenosis in certain coronary lesions, clinical trials studying the use of drug-eluting stents in peripheral artery disease have reported disappointing long-term results (6,7).

These stent-related complications led investigators to evaluate other strategies for local delivery of antiproliferative or "pro-healing" drugs without the need for an implanted drug delivery system. Such strategies may allow the delivery of a drug at therapeutic doses initially without the restriction imposed by stent-based delivery systems. We have shown that local delivery of therapeutic agents could acutely stabilize atheroma and result in durable anti-inflammatory effects against neointimal hyperplasia (8). Our delivery platform is based on an echogenic liposomal formulation with targeting capabilities via surface functionalization that can be loaded with both gaseous and hydrophilic therapeutic agents and activated with ultrasound exposure for controlled payload release. Our previous studies showed the versatility of such a delivery platform in delivering bioactive gases and other therapeutic agents that are molecularly targeted to atheroma and resulted in attenuation of neointimal hyperplasia (8), enhancing the effects of thrombolytic agents (9) and reducing the infarct size in stroke (10,11).

The current study used a combined endovascular ultrasound and delivery system approved by the US

From the [a]Department of Internal Medicine, The University of Texas Health Science Center at Houston, Houston, Texas; [b]Center for Clinical and Translational Sciences, The University of Texas Health Science Center at Houston, Houston, Texas; [c]Department of Biomedical Engineering, University of Cincinnati, Cincinnati, Ohio; [d]EKOS Corporation, Bothell, Washington; [e]Department of Pathology, Texas Heart Institute, Houston, Texas; and the [f]Department of Bio-Mechatronic Engineering, Sungkyunkwan University, Suwon, Republic of Korea. This project was supported by the National Institutes of Health (1R01HL135092). Dr. Huang is a stockholder to Zymo Pharma. Dr. Klegerman reports board service, ownership interest, and stock ownership for Zymo Pharma. Dr. Genstler is an employee and shareholder of EKOS Corporation. Dr. Haworth is a consultant for EKOS Corporation. Dr. Holland is a consultant for BTG/EKOS Corporation on another project. Dr. McPherson is a stockholder in Zymo Pharma. All other authors have reported that they have no relationships relevant to the contents of this paper to disclose.
The authors attest they are in compliance with human studies committees and animal welfare regulations of the authors' institutions and Food and Drug Administration guidelines, including patient consent where appropriate. For more information, visit the *JACC: Basic to Translational Science* author instructions page.

Manuscript received June 6, 2019; revised manuscript received September 5, 2019, accepted September 5, 2019.

Food and Drug Administration to enable site-specific delivery of therapeutic agents from echogenic liposomes (ELIPs) into stented peripheral arteries. The initial phase of ELIP infusion delivers therapeutic doses of nitric oxide (NO) for acute antioxidative and antiplatelet effects, as well as increasing arterial wall permeability to maximize drug delivery efficiency. The subsequent phase of ELIP infusion targets adhesion molecule expression in the vicinity of the stented vessels and delivers pioglitazone (PGN) into the arterial wall for sustained anti-inflammatory and antiproliferative effects. We hypothesized that such an ultrasound delivery strategy of echogenic liposomal payload would inhibit neointimal hyperplasia and in-stent restenosis in the stented peripheral arteries in a large animal model of atherosclerosis.

SEE PAGE 12

METHODS

PREPARATION AND CHARACTERIZATION OF NO-ELIPs. The preparation of ELIPs, anti-intercellular adhesion molecule-1 (ICAM-1)-conjugated ELIPs, NO-loaded ELIPs, and PGN-loaded ELIPs has been described previously (8,12–14). To prepare NO-ELIPs, lipid components, egg phosphatidylcholine, dipalmitoylphosphatidylcholine, 1,2-dioleoyl-sn-glycero-3-phosphoethanolamine, dipalmitoylphosphatidylglycerol, and cholesterol (27:42:8:8:15, molar percent) were mixed in a glass vial as chloroform solutions. The chloroform was then removed by evaporation under argon followed by vacuum overnight. The dried lipid film was rehydrated with deionized water at 10 mg of lipid per milliliter. The hydrated lipid was then incubated at 55°C for 30 min to ensure that all lipids were in the liquid crystalline phase during hydration. The mixture was then sonicated in a water bath for 5 min, following which an equal volume of 0.32 M mannitol was added. Samples of 5 mg were transferred to a 2 ml glass vial and frozen on dry ice (-80°C) for 4 h. The frozen sample was lyophilized for 48 h. After lyophilization, the vial containing the dry cake was topped with argon and capped with a lid fitted with a rubber septum. A mixture of NO (Specialty Gases of America Inc., Toledo, Ohio) and octafluoropropane (Matheson Tri-Gas, Houston, Texas) at a ratio of 1:9 was deoxygenated by bubbling through 5 M sodium hydroxide before being injected into the vial containing the lyophilized dry cake via the rubber septum. Before administration, the dry cake was reconstituted with deoxygenated water saturated with NO and octafluoropropane (1:9).

PREPARATION OF ANTIBODY-CONJUGATED PGN-ELIPs. To prepare PGN-ELIPs, lipid components, 1,2-distearoyl-sn-glycero-3-phosphocholine, 1,2-dioleoyl-sn-glycero-3-phosphoethanolamine-N-[4-(p-maleimidophenyl) butyramide], 1,2-dioleoyl-sn-glycero-3-phosphocholine, and cholesterol (52:8:30:10, molar percent) were mixed in a 250 ml round bottom flask. PGN (2 mg) was dissolved in 1 ml chloroform and added to the lipid mixture. The chloroform was removed under argon followed by vacuum overnight. The dried lipid film was hydrated with 0.32 M mannitol. The PGN-ELIPs were separated from free PGN by centrifugation at 5,800 g for 10 min.

To prepare antibody-conjugated PGN-ELIPs, 0.4 mg monoclonal anti-human/porcine ICAM-1 (Clone R6.5, eBioscience, Thermo Fisher Scientific, Waltham, Massachusetts) and 1.6 mg nonspecific mouse immunoglobulin G (IgG; Rockland Immunochemicals, Inc., Gilbertsville, Pennsylvania) were thiolated by reacting with 3-(2-pyridyldithio propionic acid)-*N*-hydroxysuccinimide ester (SPDP) at a SPDP:IgG protein molar ratio of 15:1 for 30 min at 24 ± 1°C. Protein was separated from unreacted SPDP by using gel chromatography on a 50 ml Sephadex G-50 column (MilliporeSigma, Burlington, Massachusetts) equilibrated with 0.05 M citrate-phosphate buffer at a pH of 5.5. Protein fractions were identified by using a spectrophotometric technique (Genesys 10 UV, Thermo Electron Corp., Milford, Massachusetts) at a wavelength of 280 nm, pooled and concentrated to ≤2 ml using Centricon YM-10 centrifugal filter units (MilliporeSigma).

The SPDP-activated protein was reduced in 25 mM dithiothreitol under argon for 30 min at 24 ± 1°C. The thiolated protein was isolated by using a Sephadex G-50 column, equilibrated and eluted with pH 6.7 citrate-phosphate buffer. The thiolated protein was reacted with reconstituted 1,2-dipalmitoyl-sn-glycero-3-phosphoethanolamine-N-[4-(*p*-maleimidophenyl) butyrate] (MPB-ELIPs) (10 mg lipid/ml 0.1 M phosphate buffer at a pH of 6.62) under argon overnight at 24 ± 1°C. The suspension was brought to an ionic strength of 0.1 N with 6% sodium chloride and centrifuged for 10 min at 10,000 rpm in a microfuge. Pellets were washed twice by centrifugation with 0.02 M phosphate-buffered saline, pH 7.4, resuspended in 0.1 M mannitol in reduced sodium (0.95 M) phosphate-buffered saline, pooled, and lyophilized in 5 mg lipid aliquots in vials capped with a rubber septum. The headspace of the vials were evacuated for 5 min by using a laboratory wall vacuum at -10 mm Hg, followed by pressurization with 2 ml of octafluoropropane through the rubber septum by using a 27-gauge needle. Before administration, the dry cake was reconstituted with deoxygenated water saturated with octafluoropropane.

SWINE PROCEDURE. The animal protocol was approved by the Animal Welfare Committee at the

University of Texas Health Science Center at Houston. Atherosclerotic lesions were induced in both subclavian arteries and the right common carotid artery in Yucatan miniature swine by using a combination of hyperlipidemic diet and balloon denudation. This swine model develops human-like atheroma and has a close phylogenetic relationship to humans; this model has been extensively used in translational laboratories for atheroma evaluation and therapeutic evaluation (15–19).

Our previous study had validated the lesion characteristics by using intravascular ultrasound (IVUS) and histology (20). Two weeks before balloon denudation, the animals were fed a hyperlipidemic diet containing 2% cholesterol and 15% lard. Oral aspirin (81 mg/d) was commenced 4 days before balloon denudation. On the day of balloon denudation, animals were sedated with tiletamine/zolazepam intramuscularly (4 mg/kg), intubated and ventilated, and anesthetized with inhaled isoflurane (1.5% to 3%). An incision was made in the right inguinal region, and the right femoral artery was exposed for insertion of a 6-F arterial sheath. Under fluoroscopic guidance, a 4-F Fogarty over-the-wire embolectomy catheter was introduced into both the subclavian arteries and the right carotid arteries, and an arterial segment of ~5 cm was denuded 3 times with the inflated balloon catheter. A total of 9 arteries were denuded. The left carotid artery was not manipulated. The animals were then continued on aspirin and the hyperlipidemic diet for 6 to 8 weeks. Analgesia in the form of intramuscular buprenorphine (0.05 mg/kg) was given 2 to 4 times daily for up to 1 week after each survival procedure.

Six to eight weeks after balloon denudation, the animals were sedated and anesthetized and subjected to balloon angioplasty and stent implantation in the denuded segments. An 8-F arterial sheath was inserted into the left femoral artery. Under fluoroscopic guidance, a 3.2-F Eagle Eye Platinum intravascular ultrasound catheter (Philips Healthcare, Bothell, Washington) was advanced into both the subclavian arteries and the right carotid artery to visualize the lumen and arterial wall of the denuded segments. Bare-metal stents (Boston Scientific, Maple Grove, Minnesota) measuring 6 mm × 18 mm were successfully deployed in 7 of the 9 denuded arterial segments. Immediately after stent implantation, an EndoSonic endovascular catheter (EKOS Corporation, Bothell, Washington) was advanced with the tip of the guide catheter placed just proximal to the stent and the EKOS ultrasound element within the stented segment. Two milliliters of NO-ELIPs (10 mg/ml) were administered at a constant rate (0.3 ml/min) via the catheter, followed by a 2 ml saline flush manually at approximately the same rate. Five minutes after NO-ELIP infusion, 2 ml of anti-ICAM-1/PGN-ELIPs (10 mg/ml) were administered at a constant rate (0.3 ml/min) via the catheter and then followed by a 2 ml manual saline flush. During all infusions, therapeutic ultrasound was delivered by the EKOS EndoSonic catheter using the following parameters: 9 W pulse average power, 15 ms pulse duration, 82.5 ms minimum pulse repetition interval, and 2.3 MHz center frequency.

Six arteries were randomized to be treated with NO-ELIPs + anti-ICAM-1/PGN-ELIPs with and without ultrasound (n = 3 with ultrasound; n = 3 without ultrasound). Eight weeks later, a laparotomy was performed, and an arterial sheath was inserted into the abdominal aorta. Under fluoroscopic guidance, an IVUS catheter was inserted into both the subclavian and right carotid arteries to visualize the changes in the luminal size and arterial wall thickness. After IVUS imaging, the animals were euthanized, and the arterial segments perfusion-fixed with neutral buffered formalin in situ and harvested for histological analysis.

To demonstrate payload delivery into the atherosclerotic arteries, heterozygous low-density lipoprotein receptor-deficient Yucatan miniature swine (n = 4) from Exemplar Genetics (Sioux Center, Iowa) (21,22) were fed a Western diet for 3 months and subjected to the following procedures. About 5 cm of the proximal carotid and subclavian arteries were inflated with a percutaneous balloon up to the nominal diameter of the arteries to simulate the stretching of the arteries during stent implantation. The lipid components of the ELIPs were labeled with rhodamine, and PGN was labeled with fluorescein isothiocyanate. For the infusions, the tip of the 8-F guide catheter was positioned just proximal to the inflated arterial segments and the EKOS ultrasound element within the inflated arterial segments. Fluorescently labeled ELIPs were delivered via the guide catheter into individual carotid and subclavian arteries with and without ultrasound activation. Thirty minutes after ELIP delivery, the animals were euthanized, and the treated arterial segments were harvested for fluorescence microscopy.

IVUS IMAGING ANALYSIS. IVUS signal data were used to reconstruct acoustic intensity datasets in the polar coordinate (radial vs. circumferential axes) (20). IVUS signal envelope data were collected at 1,024 data points per scan line. A total of 256 scan lines were collected along the radial direction per IVUS slice. The acoustic intensity datasets in the polar coordinate were transformed to the Cartesian

FIGURE 1 **Physical Properties and Localization of Pioglitazone in ELIPs**

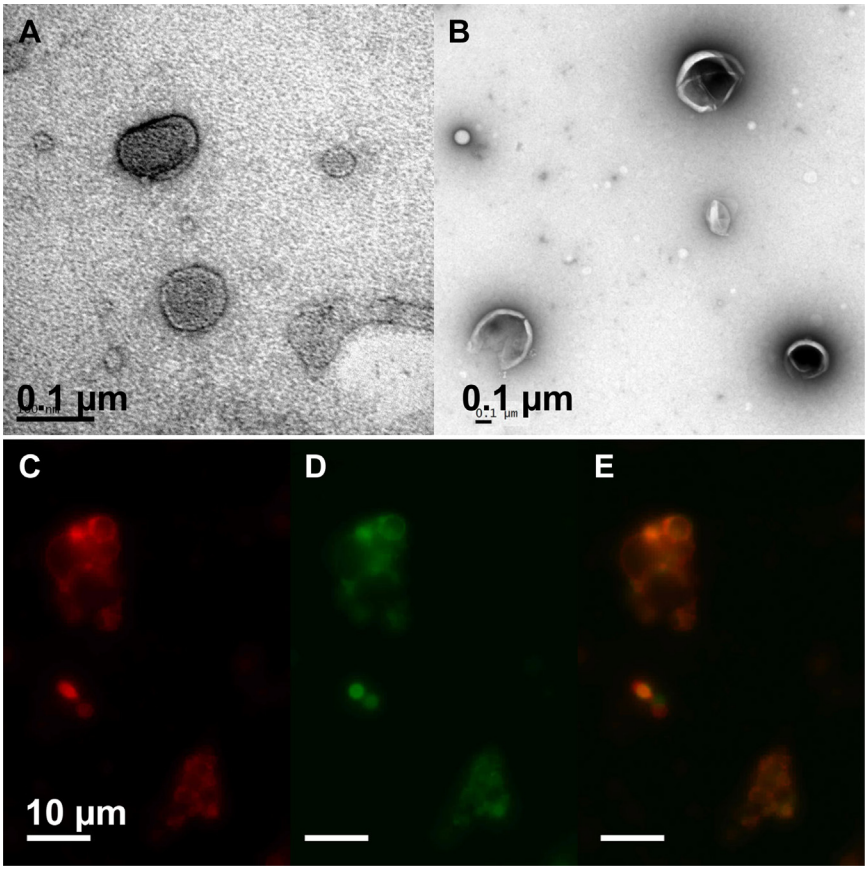

Transmission electron micrographs of **(A)** empty echogenic liposomes (ELIPs) and **(B)** ELIPs loaded with pioglitazone shown as an electron-lucency within the lipid bilayers. **(C, D, and E)** Fluorescein isothiocyanate–labeled pioglitazone **(green)** appeared to distribute within the lipid shell of the ELIPs **(red)**.

coordinate system for standard IVUS imaging. Because the imaged arterial segments of interest were relatively straight, it was assumed that the pullback direction of the IVUS catheter was parallel to the longitudinal direction of the artery. A graphical user interface-based image-processing platform was developed to interactively trace and segment the arterial structure interactively for image analysis (13,20). In a blinded manner, borders of the endothelium/atheroma and the outer edge of the dense adventitia were manually segmented in each IVUS slice. Acoustic enhancement within these arterial wall borders after each treatment was quantitated by using mean gray scale values (i.e., pixelated brightness data).

HISTOLOGICAL ANALYSIS. Arterial segments containing the stented tissue and several millimeters on either end were harvested and sent to a pathology laboratory (Alizée Pathology LLC, Thurmont, Maryland) for processing. Briefly, specimens were processed through 8 stations of graded alcohols and xylene under a program of 2 h per station. Specimens were infiltrated under the following schedule: 1) 2- to 4-h changes of acetone; 2) 48-h change in Spurr/acetone, 50/50 concentration; 3) 48-h change in Spurr 1; and 4) 48-h change in Spurr 2. Specimens were subsequently embedded in the Spurr 2 solution and placed in a 60°C oven for 48 h to polymerize. Sections were cut 5 μm thick. Two sections each were cut from the proximal, middle, and distal regions within the stented portion of each artery. In addition, 2 sections were cut from the proximal and distal regions just outside of the stented region as references. For each region, one section was stained with hematoxylin and eosin, and one section used Movat's stain for histological evaluation.

FIGURE 2 Ultrasound Facilitated the Delivery of Pioglitazone Into the Arterial Wall

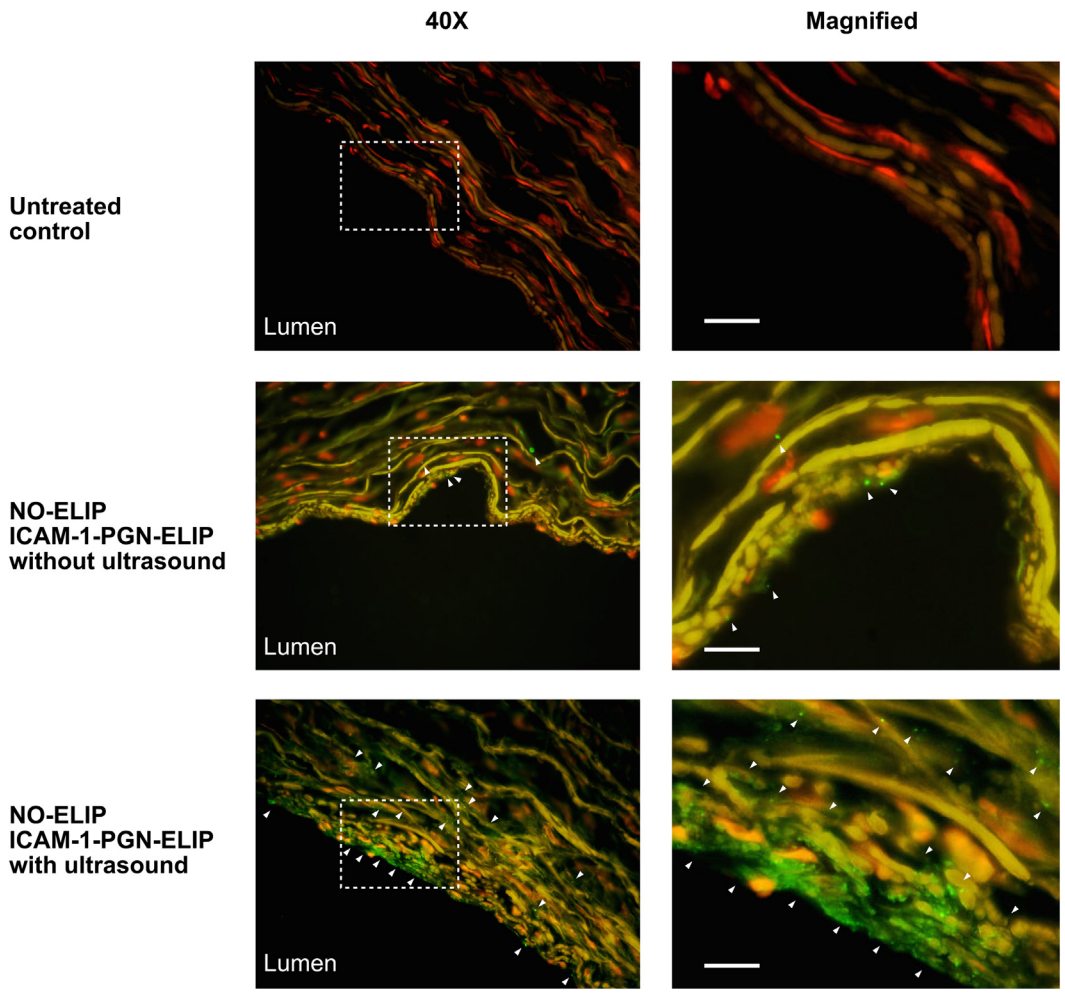

Representative images of the peripheral arteries demonstrating EKOS ultrasound-facilitated delivery of fluorescently labeled anti-intercellular adhesion molecule (ICAM)-1/pioglitazone (PGN)–echogenic liposomes (ELIPs) into the arterial wall. Multispectral imaging and secondary labeling were used with a goat anti-mouse immunoglobulin G antibody conjugated to AlexaFluor-488. Magnified sections are specified with **selection boxes**. Scale bars denote 20 μm. The extent of ELIP distribution is indicated by the **white arrows**. Without EKOS ultrasound activation **(middle)**, anti–ICAM-1/PGN-ELIPs were localized to the endothelial surface, as indicated by the **white arrows**. With EKOS ultrasound activation, anti–ICAM-1/PGN-ELIPs were seen infiltrating to at least 60 μm into the arterial wall; the **arrowheads** indicate the extent of ELIP distribution from the superficial to the deeper layers of the artery. NO = nitric oxide.

To measure the amount of neointimal hyperplasia, the intima:media ratio was measured; the outer boundary of the media (area A), the interface between the intima and the media (area B), and the lumen (area C) were manually traced with ImageJ software (National Institutes of Health, Bethesda, Maryland) in each cross-section of the arteries. The intimal volume (area B − area C) and the medial volume (area A − intimal volume) were calculated and expressed as the intima:media ratio to correct for the size and shape of various arterial segments. To show the delivery of the fluorescence payload into the artery, an AlexaFluor-488–conjugated goat anti-mouse IgG antibody at 1:800 dilution was used to detect the mouse anti-ICAM-1 antibody on the surface of anti–ICAM-1/PGN-ELIPs and imaged with the Nuance multispectral imaging system (PerkinElmer Inc., Waltham, Massachusetts).

BIOANALYTICAL ASSAY OF PGN IN ARTERIAL SEGMENTS. For bioanalytical assay, each harvested arterial segment was homogenized in 1 ml lysis buffer/100 mg tissue; 0.2 ml of each was extracted with an equal

volume of ethyl acetate. Homogenate/solvent mixtures in 1.5 ml Eppendorf microcentrifuge tubes were subjected to 2 min of vigorous vortex mixing, followed by centrifugation in a microcentrifuge (Eppendorf) for 10 min at 10,000 rpm. Twenty-microliter replicates of the ethyl acetate extracts were analyzed by isocratic high-performance liquid chromatography (Waters Corporation, Milford, Massachusetts) using a 6 × 300 mm C_{18} column and 60:40 acetonitrile/methanol mobile phase. PGN concentrations were determined relative to internal standards and normalized for tissue weight.

STATISTICAL ANALYSIS. SigmaStat (Systat Software Inc., San Jose, California) was used for statistical analyses. Student's *t*-test was used to compare the differences in neointimal volume between treatments with and without ultrasound. To account for potential correlation due to the clustered nature of data, we conducted multilevel analysis using a generalized estimating equation with an exchangeable correlation structure to compare the mean intima:media ratio and neointimal volume between the treatment and control groups. Data are represented as mean ± SEM. A p value < 0.05 was considered significant.

RESULTS

PHYSICOCHEMICAL CHARACTERISTICS OF NO-ELIPs AND ANTI–ICAM-1/PGN-ELIPs AND ENCAPSULATION EFFICIENCY OF PGN IN ELIPs. The concentration of NO in NO-ELIPs was 0.045 μmol/mg lipid. The conjugation efficiency of 3 lots of anti-ICAM-1/ELIPs subsequently loaded with PGN and used for the experiments in this study, as determined by a quantitative immunoblot assay for liposomal IgG, ranged from 0.4 to 1.8 μg antibody/mg lipid (20% of total IgG conjugated) and 137 to 422 molecules antibody/liposome, respectively (23). Beckman Coulter Multisizer 4 analysis enabled determination of both ELIP numbers and size characteristics for ELIP >0.4 μm equivalent spherical diameter, which ranged from 506 to 661 nm; ELIP numbers ranged from 4.26×10^8 to 1.23×10^{10} liposomes/mg lipid. Using transmission electron microscopy and fluorescence microscopy, the distribution of PGN was observed within the lipid bilayer in the ELIPs (Figure 1). The amount of PGN in PGN-ELIPs after anti-ICAM-1 conjugation was 39.6 μg/mg lipid.

DELIVERY OF FLUORESCENTLY LABELED ELIPs INTO THE ARTERIAL WALL. Using the Nuance multispectral imaging system, autofluorescence inherent to the elastic fibers and nuclei was still present in the control artery (Figure 2). Without ultrasound activation, anti-ICAM-1/PGN-ELIPs were observed localized to the endothelial surface of the arterial wall. With ultrasound activation, anti-ICAM-1/PGN-ELIPs were observed in the extracellular space in the deeper layers of the arterial wall.

FIGURE 3 Ultrasound-Facilitated Delivery of Pioglitazone Reduced Neointimal Atheroma Volume

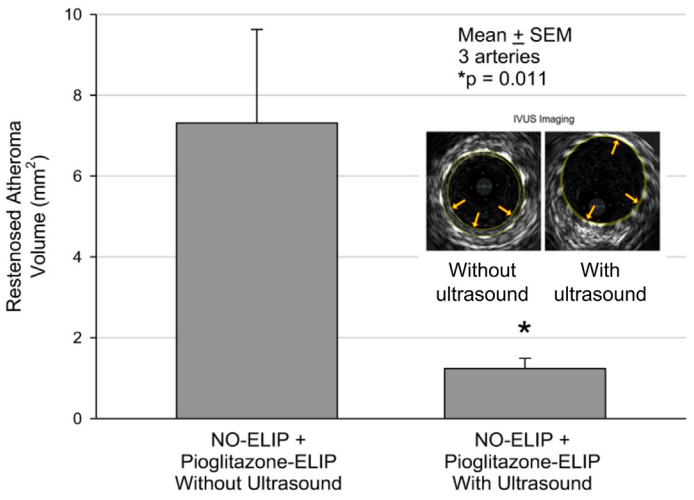

Neointimal atheroma volume within stented segments as determined by using intravascular ultrasound (IVUS). Ultrasound-facilitated delivery of ELIP payload was effective in attenuating neointimal growth within the stented arterial segments (3 stented arteries in each treatment arm). Representative IVUS images of stented segments treated with and without ultrasound are shown **(inset figure)**. Abbreviations as in Figure 2.

IVUS IMAGING. IVUS imaging revealed a reduction in the neointimal area in the stented arteries treated with NO-ELIPs and anti-ICAM-1/PGN-ELIPs with ultrasound. The mean neointimal volume in the stented arteries treated with NO-ELIPs and anti-ICAM-1/PGN-ELIPs with ultrasound activation was 1.24 ± 0.25 mm^3 (3 stented segments) and without ultrasound activation was 7.31 ± 2.32 mm^3 (3 stented segments) ($p = 0.011$) (Figure 3).

HISTOLOGICAL ANALYSIS. Histological analysis showed that neointimal formation was attenuated within the stented arteries treated with NO-ELIPs and anti-ICAM-1/PGN-ELIPs with ultrasound activation. The degree of neointimal formation was normalized to the arterial geometry by using the intima:media ratio. In the stented segments treated with NO-ELIPs and anti-ICAM-1/PGN-ELIPs with ultrasound activation, the intima:media ratio was 29.76 ± 2.26 (9 sections); without ultrasound activation, it was 46.71 ± 4.90 (9 sections) ($p < 0.001$) (Figure 4). The neointimal area of the stented arteries without ultrasound activation was 5.33 ± 1.22 μm^2; for those with

FIGURE 4 Ultrasound-Facilitated Delivery of Pioglitazone Reduced Neointimal Hyperplasia and In-Stent Restenosis

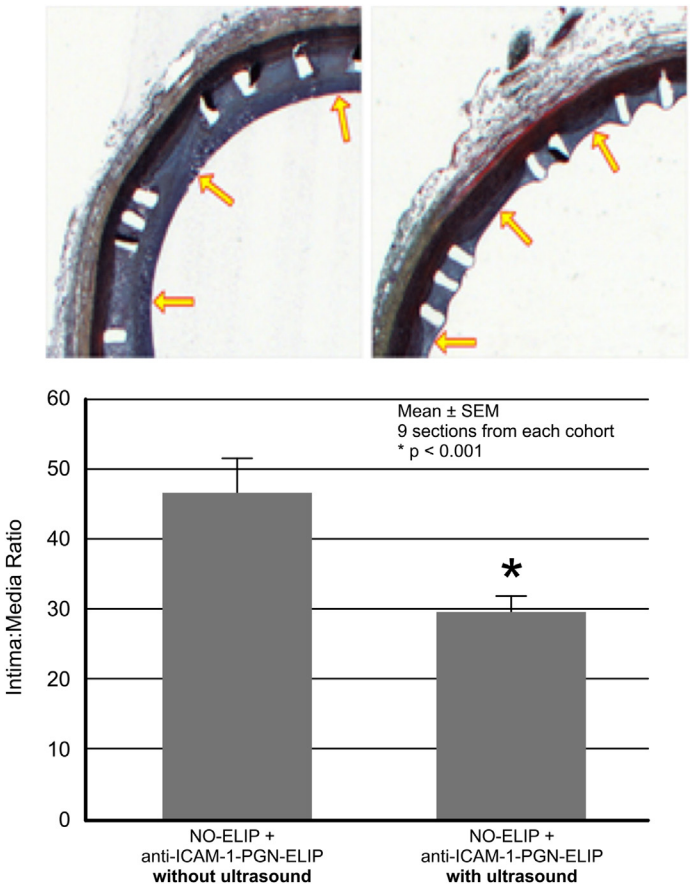

The degree of neointimal hyperplasia within stented segments was quantitated as the intima:media ratio in histological sections. Ultrasound-facilitated delivery of ELIP payload was effective in reducing neointimal growth within the stented arterial segments (9 sections from the control arteries vs. 9 sections from the treated cohort). Representative histological images of stented segments treated with and without ultrasound are shown. The **arrows** indicate the extent of neointimal formation. Abbreviations as in Figure 2.

ultrasound activation, it was 2.76 ± 0.46 μm^2 ($p = 0.0047$).

PGN BIOANALYTICAL HIGH-PERFORMANCE LIQUID CHROMATOGRAPHY. The maximal amount of PGN deposited in arterial walls by 5 mg (lipid) anti-ICAM-1/PGN-ELIPs (with NO-ELIP pretreatment and IVUS) was 6.0 ng/mg tissue, which corresponds to 14.8 μg PGN per artery, or 32.6% of the administered dose. Estimating a blood volume of 3 ml per artery, the bioavailable dose would be 4.93 μg PGN/ml or 13.8 μM. The maximally effective dose of PGN is 10 μM (24).

DISCUSSION

By using a number of innovative strategies, including ultrasound-triggered payload delivery, active molecular targeting, and combined delivery of short- and long-acting anti-inflammatory agents via ELIPs, we were able to reduce in-stent restenosis in a large animal model of atherosclerosis. A number of strategies have been recently developed to reduce in-stent restenosis. One method is to promote the dissolution of bioabsorbable stents and reduce the duration of exposure of stent components to the arterial wall. Another way is to deliver antiproliferative drugs such as sirolimus or paclitaxel by using drug-eluting stents to inhibit endothelial and smooth muscle cell proliferation. There is also a renewed interest in catheter-based therapeutic delivery at the time of intervention to overcome the limitations imposed by stent-based strategies. One example is the delivery of paclitaxel using drug-coated balloons in peripheral arterial interventions (6,7).

Our proposed approach using ultrasound-activated ELIPs aims to improve the precision and flexibility of drug delivery at the target site, and it may offer a number of potential advantages. First, the amount of drug can be modulated with minimal drug loss during transit. Second, ultrasound activation can actively deliver a precise amount of drug rather than relying on passive diffusion as in the case of drug-coated balloons. Third, a combination of therapeutic agents can be delivered concurrently (in this instance, NO for enhanced therapeutic delivery to all of the peri-stent area and PGN to stabilize the anti-inflammatory response associated with foreign body [stent] placement) to maximize both short- and long-term clinical outcomes. Finally, precision targeting by means of antibody homing enhances the retention and proximity of ELIPs at the target and improves the efficiency of ultrasound-facilitated payload delivery into the arterial wall.

Liposomes have a number of unique characteristics that are particularly suited for payload delivery (25). The compartments of aqueous core and lipid bilayer can carry both hydrophilic and lipophilic drugs, respectively. The surface of liposomes can be modified to prolong their in vivo circulation or functionalized to display homing ligands for specific targeting (16). ELIPs have the added feature of "gas pockets" that allow their visualization via ultrasound in molecular imaging (12,14,26), serve as a reservoir for bioactive gases such as NO (8), respond to ultrasound-triggered sonoporation for controlled drug release

(25), or provide nuclei for cavitation that can cause convection with enhanced drug delivery (27,28).

NO and PGN were chosen for their synergistic effects on restoring endothelial function, inhibiting inflammatory cellular recruitment and reducing neointimal hyperplasia. NO production is impaired in damaged endothelium after angioplasty and is responsible for de novo and in-stent restenosis (29,30). Stents eluting antiproliferative agents such as sirolimus and paclitaxel are more deleterious than bare-metal stents in impairing endothelium-dependent relaxation responses to acetylcholine, reducing endothelial NO synthase expression and local NO production (31,32). These effects lead to a failure of re-endothelialization and vascular repair, and they account for the high rates of very late stent thrombosis in association with drug-eluting stent implantation (5).

Incorporation and local release of NO-releasing substances via stent struts may reduce platelet adhesion and intimal hyperplasia but do not solve the issues of long-term exposure to stent components. One approach to restoring local NO production is to increase local NO synthase (NOS) activity. Adenovirus-mediated NOS gene transfer restored NO production and reduced neointima formation after angioplasty (33–35). However, longevity of gene expression and toxic effects of vector-induced inflammation are the main concerns regarding gene transfer vector technology.

Direct delivery of NO to the arterial wall is an attractive approach, as this strategy does not reduce generation of endothelial NOS uncoupling-dependent reactive oxygen species. The effective dose of NO delivery to the arterial wall can be tuned by varying the amount and rate of NO-ELIP infusion and adjusting the ultrasound parameters to control payload release. Our previous study found that NO-ELIPs can protect NO from hemoglobin scavenging and deliver NO into the rabbit artery ex vivo by using a flow circuit that mimics the flow situation inside an artery (36). However, the acute effect of NO is short-lived, and an additional agent is necessary to sustain an environment for promoting re-endothelialization and reducing local inflammation. Peroxisome proliferator-activated receptor-γ agonists such as PGN exert their pleiotropic effects at a gene level via their binding to the peroxisome proliferator response element. Peroxisome proliferator-activated receptor-γ activation plays an important role in promoting endothelial proliferation by reducing the production of plasminogen activator inhibitor type 1 (37), reducing leukocyte infiltration by suppressing adhesion molecule expression in the endothelial cells (38,39), inhibiting vascular smooth muscle migration by controlling the mitogen-activated protein kinase pathway (40,41), and reducing inflammation by attenuating cytokine production and nuclear factor-κB transcription activity (38,42). We have shown that ELIPs containing both NO and rosiglitazone could attenuate intimal proliferation in balloon-injured carotid arteries in rabbits (43).

In the current study, we improved the efficiency of ELIP-mediated payload delivery by direct intravascular delivery of the therapeutic agents, active targeting of the ELIPs to the inflamed endothelium with anti-ICAM-1 antibody targeting, and site-specific ultrasound-activated payload release using the EKOS catheter. Bioanalytical determination of PGN concentrations in arterial homogenates confirmed deposition of the drug in the arterial wall at an equivalent concentration within the effective range (24). Because this mode of PGN delivery is different from the water-soluble plasma distribution seen in current practice, pharmacodynamic studies are needed to confirm that the delivered dose is sufficient to provoke the desired anti-inflammatory effects. Evidence for treatment efficacy provided by this study, however, is consistent with that hypothesis. In our previous study, we showed that ultrasound activation was effective in delivering calcein-loaded immunoliposomes into all layers of the arterial wall in a miniature swine model (44).

STUDY LIMITATIONS. Although we evaluated 9 arteries, each artery was segmented into multiple sections, yielding additional data points for IVUS and histological analyses. Fixed doses of NO and PGN, as well as one ultrasound parameter, were studied. Optimization of the delivery strategy is still required. NO-ELIPs and anti-ICAM-1/PGN-ELIPs were not tested independently for their therapeutic effects in the current study. However, we have evidence that pre-treatment of the artery with NO-ELIPs was absolutely necessary to facilitate the subsequent delivery of anti-ICAM-1/ELIPs into the arterial wall (14). Ideally, both ELIPs should be tested independently, but we decided that resources were better used to evaluate the effect of ultrasound activation in drug delivery. Oral PGN was not considered as a control because the objective of this study was to evaluate local intra-arterial delivery of the therapeutic agents during stent implantation for acute reduction in inflammation and avoid the systemic side effects of the agent.

The major advantage of our PGN formulation is the much lower dose of the drug to be administered than what is administered systemically, probably obviating the adverse effects previously seen in clinical use of the drug. Although we reported evidence of payload delivery into the arterial wall, the exact amount of payload delivery has not been determined. Another consideration relates to the relatively short duration (8 weeks) between stent implantation and tissue harvest for histological analysis. As a result, future studies must be performed to show the durable effect of this therapeutic approach in preventing late restenosis. Finally, although the Yucatan miniature swine model of atherosclerosis generates human-like atheroma and has been widely used as a pre-clinical model for device and drug evaluation, the lesions may not resemble all chronic pathobiological features and natural history seen in human atherosclerosis. The size and anatomical similarity of the animal with humans make it a valuable tool for evaluation of intravascular devices for drug delivery.

CONCLUSIONS

A combined strategy of active targeting and ultrasound-facilitated delivery of NO and PGN was effective in attenuating neointimal growth and in-stent restenosis in stented peripheral arteries. These findings set the stage for further development of the drug delivery ultrasound catheter for direct therapy for multiple atheromatous vascular territories.

ADDRESS FOR CORRESPONDENCE: Dr. Patrick H. Kee, Department of Internal Medicine, The University of Texas Health Science Center at Houston, 1881 East Road, 3SCRB 6.4607, Houston, Texas 77054-6011. E-mail: patrick.kee@uth.tmc.edu.

PERSPECTIVES

COMPETENCY IN MEDICAL KNOWLEDGE: In-stent restenosis remains a major clinical issue even in the era of drug-eluting stents. We used an ultrasound-triggered drug delivery system approved by the U.S. Food and Drug Administration to deliver our novel drug-loaded ELIPs deployable at the time of stent implantation. Such a treatment strategy attenuated neointimal formation in the stented peripheral arteries in a large animal model of atherosclerosis and represents a promising approach to the management of in-stent restenosis.

TRANSLATIONAL OUTLOOK: For the clinical translation, first-in-human study will be carried out in human subjects with obstructive peripheral artery disease requiring stent implantation. Ultrasound-facilitated delivery of NO and PGN will be performed immediately after stent implantation. Safety, symptomatic improvement and functional improvement will be evaluated in the subjects.

REFERENCES

1. Abdulhannan P, Russell DA, Homer-Vanniasinkam S. Peripheral arterial disease: a literature review. Br Med Bull 2012;104:21–39.

2. Brower V. Stents and biology combination for restenosis. Nat Biotechnol 1996;14:422.

3. Farb A, Weber DK, Kolodgie FD, Burke AP, Virmani R. Morphological predictors of restenosis after coronary stenting in humans. Circulation 2002;105:2974–80.

4. Finn AV, Nakazawa G, Joner M, et al. Vascular responses to drug eluting stents: importance of delayed healing. Arterioscler Thromb Vasc Biol 2007;27:1500–10.

5. Nakazawa G, Vorpahl M, Finn AV, Narula J, Virmani R. One step forward and two steps back with drug-eluting-stents: from preventing restenosis to causing late thrombosis and nouveau atherosclerosis. J Am Coll Cardiol Img 2009;2:625–8.

6. Duda SH, Pusich B, Richter G, et al. Sirolimus-eluting stents for the treatment of obstructive superficial femoral artery disease: six-month results. Circulation 2002;106:1505–9.

7. Duda SH, Bosiers M, Lammer J, et al. Sirolimus-eluting versus bare nitinol stent for obstructive superficial femoral artery disease: the SIROCCO II trial. J Vasc Interv Radiol 2005;16:331–8.

8. Huang SL, Kee PH, Kim H, et al. Nitric oxide-loaded echogenic liposomes for nitric oxide delivery and inhibition of intimal hyperplasia. J Am Coll Cardiol 2009;54:652–9.

9. Laing ST, Moody MR, Kim H, et al. Thrombolytic efficacy of tissue plasminogen activator-loaded echogenic liposomes in a rabbit thrombus model. Thromb Res 2012;130:629–35.

10. Peng T, Britton GL, Kim H, et al. Therapeutic time window and dose dependence of xenon delivered via echogenic liposomes for neuroprotection in stroke. CNS Neurosci Ther 2013;19:773–84.

11. Kim H, Britton GL, Peng T, Holland CK, McPherson DD, Huang SL. Nitric oxide-loaded echogenic liposomes for treatment of vasospasm following subarachnoid hemorrhage. Int J Nanomedicine 2014;9:155–65.

12. Hamilton AJ, Huang SL, Warnick D, et al. Intravascular ultrasound molecular imaging of atheroma components in vivo. J Am Coll Cardiol 2004;43:453–60.

13. Kim H, Kee PH, Rim Y, et al. Nitric oxide improves molecular imaging of inflammatory atheroma using targeted echogenic immunoliposomes. Atherosclerosis 2013;231:252–60.

14. Kee PH, Kim H, Huang S, et al. Nitric oxide pretreatment enhances atheroma component highlighting in vivo with intercellular adhesion molecule-1-targeted echogenic liposomes. Ultrasound Med Biol 2014;40:1167–76.

15. Reitman JS, Mahley RW, Fry DL. Yucatan miniature swine as a model for diet-induced atherosclerosis. Atherosclerosis 1982;43:119–32.

16. Gal D, Rongione AJ, Slovenkai GA, et al. Atherosclerotic Yucatan microswine: an animal model with high-grade, fibrocalcific, nonfatty lesions suitable for testing catheter-based interventions. Am Heart J 1990;119:291–300.

17. Barbeau ML, Klemp KF, Guyton JR, Rogers KA. Dietary fish oil. Influence on lesion regression in

the porcine model of atherosclerosis. Arterioscler Thromb Vasc Biol 1997;17:688–94.

18. de Smet BJ, Pasterkamp G, van der Helm YJ, Borst C, Post MJ. The relation between de novo atherosclerosis remodeling and angioplasty-induced remodeling in an atherosclerotic Yucatan micropig model. Arterioscler Thromb Vasc Biol 1998;18:702–7.

19. de Smet BJ, van der Zande J, van der Helm YJ, Kuntz RE, Borst C, Post MJ. The atherosclerotic Yucatan animal model to study the arterial response after balloon angioplasty: the natural history of remodeling. Cardiovasc Res 1998;39:224–32.

20. Kim H, Moody MR, Laing ST, et al. In vivo volumetric intravascular ultrasound visualization of early/inflammatory arterial atheroma using targeted echogenic immunoliposomes. Invest Radiol 2010;45:685–91.

21. Davis BT, Wang XJ, Rohret JA, et al. Targeted disruption of LDLR causes hypercholesterolemia and atherosclerosis in Yucatan miniature pigs. PLoS One 2014;9:e93457.

22. Burke AC, Telford DE, Sutherland BG, et al. Bempedoic acid lowers low-density lipoprotein cholesterol and attenuates atherosclerosis in low-density lipoprotein receptor-deficient (LDLR(+/-) and LDLR(-/-)) Yucatan miniature pigs. Arterioscler Thromb Vasc Biol 2018;38:1178–90.

23. Klegerman ME, Hamilton AJ, Huang SL, et al. Quantitative immunoblot assay for assessment of liposomal antibody conjugation efficiency. Anal Biochem 2002;300:46–52.

24. Orasanu G, Ziouzenkova O, Devchand PR, et al. The peroxisome proliferator-activated receptor-gamma agonist pioglitazone represses inflammation in a peroxisome proliferator-activated receptor-alpha-dependent manner in vitro and in vivo in mice. J Am Coll Cardiol 2008;52:869–81.

25. Huang S, Hamilton AJ, Tiukinhoy SD, et al. Liposomes as ultrasound imaging contrast agents and as ultrasound-sensitive drug delivery agents. Cell Mol Biol Lett 2002;7:233–5.

26. Huang SL, Hamilton AJ, Pozharski E, et al. Physical correlates of the ultrasonic reflectivity of lipid dispersions suitable as diagnostic contrast agents. Ultrasound Med Biol 2002;28:339–48.

27. Sutton JT, Haworth KJ, Pyne-Geithman G, Holland CK. Ultrasound-mediated drug delivery for cardiovascular disease. Expert Opin Drug Deliv 2013;10:573–92.

28. Haworth KJ, Raymond JL, Radhakrishnan K, et al. Trans-stent B-mode ultrasound and passive cavitation imaging. Ultrasound Med Biol 2016;42:518–27.

29. Myers PR, Webel R, Thondapu V, et al. Restenosis is associated with decreased coronary artery nitric oxide synthase. Int J Cardiol 1996;55:183–91.

30. Piatti P, Di Mario C, Monti LD, et al. Association of insulin resistance, hyperleptinemia, and impaired nitric oxide release with in-stent restenosis in patients undergoing coronary stenting. Circulation 2003;108:2074–81.

31. Shin DI, Kim PJ, Seung KB, et al. Drug-eluting stent implantation could be associated with long-term coronary endothelial dysfunction. Int Heart J 2007;48:553–67.

32. Togni M, Raber L, Cocchia R, et al. Local vascular dysfunction after coronary paclitaxel-eluting stent implantation. Int J Cardiol 2007;120:212–20.

33. Janssens S, Flaherty D, Nong Z, et al. Human endothelial nitric oxide synthase gene transfer inhibits vascular smooth muscle cell proliferation and neointima formation after balloon injury in rats. Circulation 1998;97:1274–81.

34. Varenne O, Pislaru S, Gillijns H, et al. Local adenovirus-mediated transfer of human endothelial nitric oxide synthase reduces luminal narrowing after coronary angioplasty in pigs. Circulation 1998;98:919–26.

35. von der Thusen JH, Fekkes ML, Passier R, et al. Adenoviral transfer of endothelial nitric oxide synthase attenuates lesion formation in a novel murine model of postangioplasty restenosis. Arterioscler Thromb Vasc Biol 2004;24:357–62.

36. Chrzanowski SM, Kim H, McPherson D, Huang S. Ultrasound triggered nitric oxide release from echogenic liposomes improves arterial vasodilation. Circulation 2018;118:S_465.

37. Hong HK, Cho YM, Park KH, Lee CT, Lee HK, Park KS. Peroxisome proliferator-activated receptor gamma mediated inhibition of plasminogen activator inhibitor type 1 production and proliferation of human umbilical vein endothelial cells. Diabetes Res Clin Pract 2003;62:1–8.

38. Jackson SM, Parhami F, Xi XP, et al. Peroxisome proliferator-activated receptor activators target human endothelial cells to inhibit leukocyte-endothelial cell interaction. Arterioscler Thromb Vasc Biol 1999;19:2094–104.

39. Wang N, Verna L, Chen NG, et al. Constitutive activation of peroxisome proliferator-activated receptor-gamma suppresses pro-inflammatory adhesion molecules in human vascular endothelial cells. J Biol Chem 2002;277:34176–81.

40. Ricote M, Li AC, Willson TM, Kelly CJ, Glass CK. The peroxisome proliferator-activated receptor-gamma is a negative regulator of macrophage activation. Nature 1998;391:79–82.

41. Goetze S, Xi XP, Kawano H, et al. PPAR gamma-ligands inhibit migration mediated by multiple chemoattractants in vascular smooth muscle cells. J Cardiovasc Pharmacol 1999;33:798–806.

42. Jiang C, Ting AT, Seed B. PPAR-gamma agonists inhibit production of monocyte inflammatory cytokines. Nature 1998;391:82–6.

43. Moody MR, Huang S, Kim H, Chrzanowski S, McPherson DD. Abstract 5552: bioactive gas/drug co-encapsulation and release improve attenuation of intimal hyperplasmia following acute arterial injury. Circulation 2016;118:S_573.

44. Laing ST, Kim H, Kopechek JA, et al. Ultrasound-mediated delivery of echogenic immunoliposomes to porcine vascular smooth muscle cells in vivo. J Liposome Res 2010;20:160–7.

KEY WORDS **atherosclerosis, in-stent restenosis, nitric oxide, pioglitazone, ultrasound contrast agent**